ENGINEERING TRANSACTIONS • *Engng. Trans.* • **52**, 1-2, 5–22, 2004
Polish Academy of Sciences • Institute of Fundamental Technological Research
10.24423/engtrans.466.2004

ANALYSIS OF LOAD-CAPACITY AT COLLAPSE OF I-SECTION THIN-WALLED BEAM

S. Gawłowski, R. B. Pęcherski

Institute of Structural Mechanics
Cracow University of Technology,
Warszawska 24, 31-155 Cracow, Poland
e-mail: sg@limba.wil.pk.edu.pl

The aim of the paper is to analyse the load-capacity at collapse for thin-walled beams under the assumption of static approach. I-section beams subjected to torsion and bending with torsion are studied. The general formula for an interaction surface was derived. The comparison of the examples solved analytically with the finite element calculations and experimental results confirms the assumed hypotheses concerning statically admissible distribution of stresses in a plastic hinge. The analysis revealed also that normal stresses have a decisive influence on the value of load-carrying capacity in the case of thin-walled beams.

Key words: thin-walled beam, load-capacity at collapse, interaction surface.

1. Introduction

The presented analytic approach is based on the thin-walled beam theory formulated by Vlasov [1]. The static models of plastic hinge, which are used in the paper and a general algorithm of determination of load-capacity at collapse for thin-walled beams, are based on the work of Strel'bitskaya [2]. The presented formulae are derived in accordance with the new approach to thin-walled beams theory given in Piechnik [3]. It means that all variables are defined in the local co-ordinate system related to the middle line of cross-section. The experimental data, which are used in the analysis, are taken from Strel'bitskaya and Ievsieienko [4]. The basic information of theory of plasticity that is necessary for solution of the considered problem is given in the monographs of Życzkowski [5] and Heyman [6]. The former one provides also comprehensive overview of the works related with elastic-plastic analysis of thin-walled beams. The contribution of Gawłowski and Piechnik [7] presents details of the algorithm, which leads to analytic determination of the static and kinematic quantities for thin-walled beams. It shows in particular a new way of definition of the

boundary conditions. Numerical modelling of thin-walled beams was presented e.g. in BATHE and WIENER [8] and RAMM and OSTERRIEDER [9]. The recent works, which analyse the behaviour of thin-walled beams beyond the elastic range are IZZUDDIN and LLOYD SMITH [10], MURRAY [11] and KOTEŁKO [12]. The first paper presents distributions of normal and shear stresses in elastic-plastic state. The stress diagrams are created, however, especially for numerical application and are not used for determination of the load-capacity at collapse. Two remaining contributions deal with kinematic approach to the problem of calculation of the load-carrying capacity for thin-walled beams. It appears that static approach has not been studied so intensively as the kinematic one. This encourages the authors to develop the static method, which can give the better insight into the limit analysis and provides lower estimate of load-capacity at collapse.

2. MAIN ASSUMPTIONS

The presented study is based on the VLASOV thin-walled beams theory [1]. The Vlasov hypothesis results in a new cross-sectional forces: bimoment – B_ω, Vlasov torsion moment – M_ω and Saint–Venant torsion moment (torque) – M_s.

Following [3], it is assumed that two co-ordinate systems are used, the global one (xyz), and the local one (xsn), which appear to be helpful in the analysis of thin-walled beams – Fig. 1. The components of stress tensor are defined in the local system.

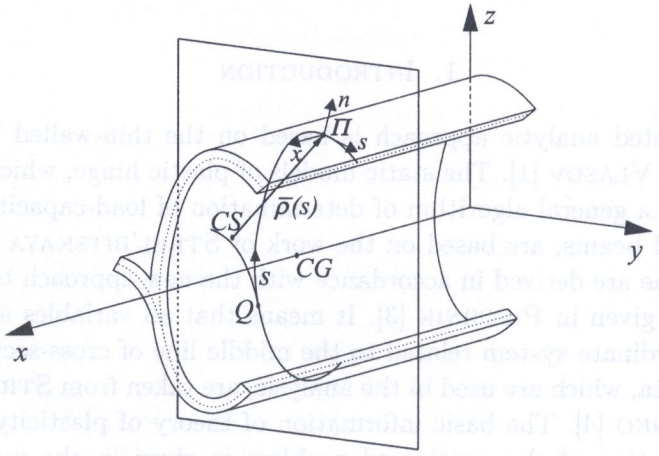

FIG. 1.

The x-axis of the global system is the beam centre line, while the y and z-axes are the principal axes of the cross-section. Therefore the point CG is the cross-section centre of gravity. The system xsn can be defined at any point Π of

the middle surface. The x-axis of the local co-ordinate system is parallel to the beam centre line, the s-axis is tangential to the middle line, and the n-axis is perpendicular to the x and s-axes. The natural co-ordinate s is measured from point Q. CS denotes the shear centre and also the origin of vector $\bar{\rho}$, which determines the locus of point Π. For the analysed bisymmetrical I-section, the points CS and Q coincide with the cross-section centre of gravity CG.

In further analysis, the elastic-ideally-plastic material with the Huber–Mises–Hencky yield criterion is considered. For thin-walled beams the yield condition reads

$$\sigma_x^2 + 3\tau_{xs}^2 = \sigma_Y^2, \tag{2.1}$$

where σ_Y is the tensile yield limit.

It should also be mentioned that the diagrams of statically admissible normal and shear stresses in plastic hinge are assumed as rectangles.

Buckling is not included, what restricts the presented considerations to the cases of cross-sections with limited slenderness ratios of legs.

3. Interaction surface for bending and torsion of I-section thin-walled beam

Taking the diagrams of normal – σ_x and shear – τ_{xs} stress components for bending and torsion of I-section thin-walled beam in elastic state as a motivation, the distributions of statically admissible stresses in the plastic hinge for the considered case are assumed in the form depicted in Fig. 2.

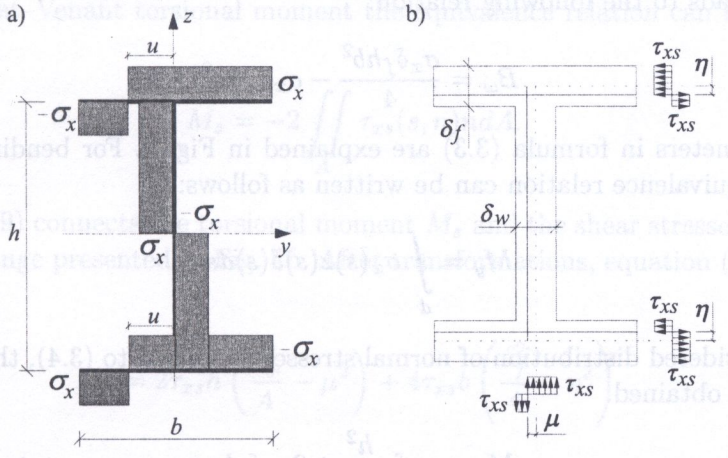

Fig. 2.

It is important to note that in this study the cross-sectional forces that all have positive values generate the assumed diagrams of stress distribution. Oth-

erwise, the inconsistencies by the derivation of interaction surface appear. For example, in the interaction surface formula of (STREL'BITSKAYA [2]) the discontinuities can be detected.

In the considered problem the following five cross-sectional forces appear: bimoment – B_ω and bending moment – M_y, which induce normal stresses, and also the Vlasov torsional moment – M_ω, Saint–Venant torsional moment – M_s and shear force – F_z, which generate shear stresses. As a result, the general form of interaction surface formula can be written as follows:

$$f(B_\omega, M_y, M_\omega, M_s, F_z) = 1. \tag{3.1}$$

In order to derive the interaction surface formula, the relations between cross-sectional forces and pertinent stress components should be found. Application of the concept of kinematical equivalence of the system of external and internal (cross-sectional) forces presented in [3] enables us to derive the suitable expressions. In the case of a bimoment, the equivalence relation assumes the form

$$B_\omega = \int_d \sigma_x(s)\omega(s)\delta(s)ds. \tag{3.2}$$

Formula (3.2) presents a curvilinear integral over the whole middle line d of the cross-section. In the general approach presented in [3] the concepts of graph theory are applied. In such a case the integral (3.2) is calculated over the dendrite d. Function $\omega(s)$ is a sectorial co-ordinate, whereas $\delta(s)$ denotes the cross-section thickness. Application of Eq. (3.2) for the diagram of normal stresses, given in Fig. 2a, leads to the following relation:

$$B_\omega = \frac{\sigma_x \delta_f h b^2}{4} - \sigma_x \delta_f h u^2. \tag{3.3}$$

The parameters in formula (3.3) are explained in Fig. 2. For bending moment M_y the equivalence relation can be written as follows:

$$M_y = \int_d \sigma_x(s)z(s)\delta(s)ds. \tag{3.4}$$

If the considered distribution of normal stresses is applied to (3.4), the following relation is obtained:

$$M_y = \sigma_x \delta_w \frac{h^2}{4} + 2\sigma_x \delta_f h u. \tag{3.5}$$

Both the equations (3.3) and (3.5) contain the parameter u, which determines the distribution of normal stresses. This quantity can be eliminated from the

equivalence relations what leads to a quadratic equation for σ_x, the solution of which reads

$$\sigma_x = \frac{B_\omega - \frac{M_y \delta_w h}{8\delta_f} + \sqrt{B_\omega^2 - \frac{B_\omega M_y \delta_w h}{4\delta_f} + \frac{M_y^2 b^2}{4}}}{\frac{\delta_f h b^2}{2} - \frac{\delta_w^2 h^3}{32\delta_f}}. \tag{3.6}$$

This gives the value of normal stress for limit state.

In order to find the expression for shear stress τ_{xs} in the limit state, the following analysis is made. In the case of Vlasov torsional moment, the equivalence relation has the form [3]:

$$M_\omega = -\iint_A \tau_{xs}(s,n)\rho_n(s)dA. \tag{3.7}$$

In formula (3.7), the double integral over the whole cross-section is used, because the variation of the shear stresses across the thickness of thin-walled cross-section should not be neglected. The quantity ρ_n denotes projection of the vector $\bar{\rho}$ on direction n. Application of the shear stress distribution from Fig. 2b in expression (3.7) leads to:

$$M_\omega = 2\tau_{xs} h b \eta. \tag{3.8}$$

For the Saint–Venant torsional moment the equivalence relation can be written as follows:

$$M_s = -2\iint_A \tau_{xs}(s,n) n dA. \tag{3.9}$$

Formula (3.9) connects the torsional moment M_s and the shear stresses diagram in plastic hinge presented in Fig. 2b. After transformations, equation (3.9) takes the form:

$$M_s = 2\tau_{xs} h \left(\frac{\delta_w^2}{4} - \mu^2\right) + 4\tau_{xs} b \left(\frac{\delta_f^2}{4} - \eta^2\right). \tag{3.10}$$

In the case of shear force F_z, the equivalence relation reads:

$$F_z = \iint_A \tau_{xs}(s,n)\dot{z}(s)dA. \tag{3.11}$$

The quantity $\dot{z}(s)$ in the above relation is a derivative with respect to the s co-ordinate of the function $z(s)$. For the analysed problem, expression (3.11) assumes the form:

$$F_z = 2\tau_{xs} h \mu. \tag{3.12}$$

From Eqs. (3.8) and (3.12), values η and μ, which define the diagram of shear stresses in plastic hinge, can be calculated. Substitution of these quantities to (3.10) leads to the quadratic equation for τ_{xs}, the solution of which has the form:

$$\tau_{xs} = \frac{M_s + \sqrt{M_s^2 + 4\left(h\frac{\delta_w^2}{2} + b\delta_f^2\right)\left(\frac{F_z^2}{2h} + \frac{M_\omega^2}{bh^2}\right)}}{2\left(h\frac{\delta_w^2}{2} + b\delta_f^2\right)}. \tag{3.13}$$

Expressions (3.6) and (3.13) determine the values of normal and shear stresses in the plastic hinge. It means that if both stresses will be substituted to the yield criterion (2.1), the interaction surface formula will be obtained. After transformations, this interaction surface formula assumes the following form:

$$\frac{M_s^2}{2M_{sY}^2} + \sqrt{\frac{M_s^4}{4M_{sY}^4} + \frac{M_s^2}{M_{sY}^3}\frac{\sigma_Y}{\sqrt{3}}\left[\frac{F_z^2}{2h} + \frac{M_\omega^2}{bh^2}\right] + \frac{1}{M_{sY}}\frac{\sigma_Y}{\sqrt{3}}\left[\frac{F_z^2}{2h} + \frac{M_\omega^2}{bh^2}\right]} + 2\frac{(B_\omega - DM_y)^2}{R^2\sigma_Y^2} + 2\sqrt{\frac{(B_\omega - DM_y)^4}{R^4\sigma_Y^4} + \frac{(B_\omega - DM_y)^2 M_y^2}{R^2 S\sigma_Y^4} + \frac{M_y^2}{S\sigma_Y^2}} = 1, \tag{3.14}$$

where $M_{sY} = \frac{\sigma_Y}{\sqrt{3}}\left(\frac{h\delta_w^2}{2} + b\delta_f^2\right)$ is the limit value of Saint–Venant moment,

$$D = \frac{\delta_w h}{8\delta_f}, \qquad R = \frac{\delta_f h b^2}{2} - \frac{\delta_w^2 h^3}{32\delta_f}, \qquad S = \delta_f^2 h^2 b^2 - \frac{\delta_w^2 h^4}{16}.$$

It should be underlined that Eq. (3.14) is a new result, which correctly describes the interaction surface for the considered case.

4. Numerical example – bending and torsion of I-section thin-walled beam

The numerical example for cantilever I-section beam shown in Fig. 3 will be solved. The boundary conditions are idealised by means of the constraints imposed upon the six degrees of freedom of the body and additionally, upon the warping of the cross-section.

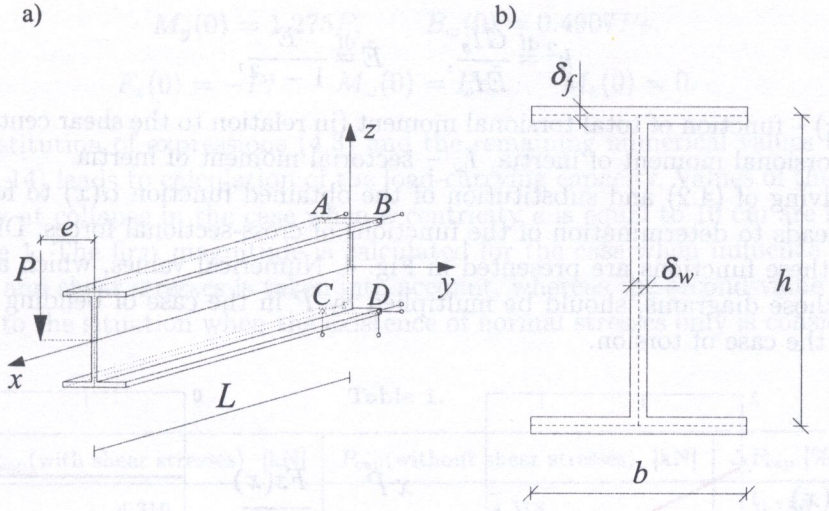

FIG. 3.

The load-capacity at collapse will be determined for the following numerical data:

Data: Length of beam: $L = 1.275$ m, material constants: $E = 210$ GPa, $G = 80$ GPa, $\nu = 0.3$, dimensions of cross-section – Fig. 3b: $h = 11.4$ cm, $b = 7.4$ cm, $\delta_f = 0.6$ cm, $\delta_w = 0.5$ cm, yield stress: $\sigma_Y = 231.4$ MPa.

First of all the most exerted cross-section should be found. It will determine the place where plastic hinge will appear. To this end the functions of all cross-sectional forces should be analysed. The way of calculation of the bending moment $M_y(x)$ and shear force $F_z(x)$ functions is the same as that used in the solid beam theory and is well known. The remaining relations are obtained from the following differential equations [3]:

$$
\begin{aligned}
B_\omega(x) &= \tilde{E} I_\omega \alpha''(x), \\
M_\omega(x) &= -\tilde{E} I_\omega \alpha'''(x), \\
M_s(x) &= G I_s \alpha'(x).
\end{aligned}
\tag{4.1}
$$

Function $\alpha(x)$ in expressions (4.1) describes changes of the angle of rotation of the cross-section along the beam axis. This function is a solution of the differential equation (4.2), which plays the crucial role in the Vlasov thin-walled beams theory

$$
\alpha'''(x) - k^2 \alpha'(x) = -\frac{1}{\tilde{E} I_\omega} M_x^{cs}(x),
\tag{4.2}
$$

where

$$k^2 \stackrel{\text{df}}{=} \frac{GI_s}{\tilde{E}I_\omega}, \qquad \tilde{E} \stackrel{\text{df}}{=} \frac{E}{1-\nu^2},$$

$M_x^{cs}(x)$ – function of total torsional moment (in relation to the shear centre CS), I_s – torsional moment of inertia, I_ω – sectorial moment of inertia.

Solving of (4.2) and substitution of the obtained function $\alpha(x)$ to formulae (4.1) leads to determination of the functions of cross-sectional forces. Diagrams of all these functions are presented in Fig. 4. Numerical values, which are read from those diagrams, should be multiplied by P in the case of bending and by Pe in the case of torsion.

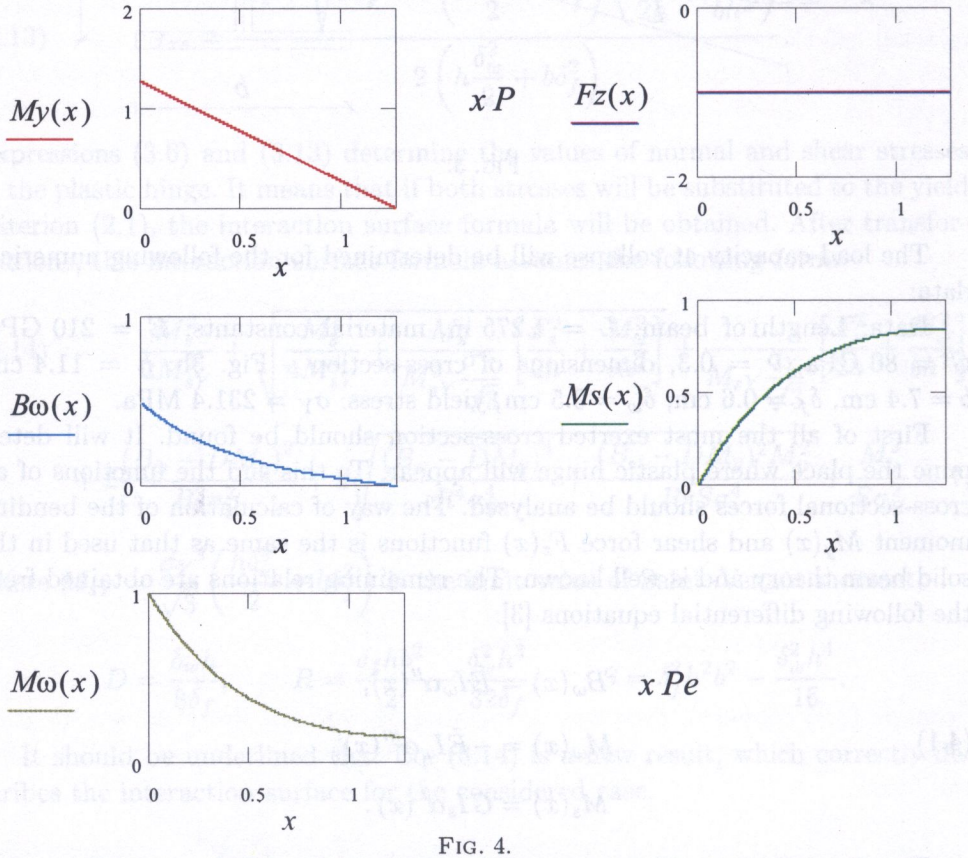

FIG. 4.

It appears that the most exerted cross-section corresponds to $x = 0$. It means that the plastic hinge appears in the fixed end of beam. At this point, the bending moment, bimoment and Vlasov torsional moment assume maximum values. Precise values of all cross-sectional forces in the plastic hinge are presented by Eq. (4.3).

$$M_y(0) = 1.275P, \qquad B_\omega(0) = 0.4907Pe,$$
$$F_z(0) = -P, \qquad M_\omega(0) = Pe, \qquad M_s(0) = 0. \tag{4.3}$$

Substitution of expressions (4.3) and the remaining numerical values to formula (3.14) leads to calculation of the load-carrying capacity. Values of the load-capacity at collapse in the case when eccentricity e is equal to 10 cm are shown in Table 1. The first magnitude is calculated for the case when influence of the normal and shear stresses is taken into account, whereas the second value corresponds to the situation when the existence of normal stresses only is considered.

Table 1.

P_{cap}(with shear stresses) [kN]	P_{cap}(without shear stresses) [kN]	ΔP_{cap} [%]
4.310	4.318	0.186

The difference between the values of load-capacity at collapse – ΔP_{cap} is very small what shows that the influence of shear stresses on the value of load-carrying capacity is negligible.

Load-capacity at collapse is also calculated for $e = 4$ cm. This value is confronted with the experimental data given by Strel'bitskaya (STREL'BITSKAYA and IEVSIEIENKO [4]) – Table 2.

Table 2.

$P_{\text{cap}}^{\text{anal}}$ [kN]	$P_{\text{cap}}^{\text{expe}}$ [kN]	ΔP_{cap} [%]
8.830	9.316	5.501

The difference ΔP_{cap} is not a large value, what confirms correctness of the considered analytical approach.

The numerical example (for eccentricity $e = 10$ cm) is also analysed by using a finite element system (ABAQUS [13]). The beam is loaded by a concentrated force, the value of which is equal to the load-carrying capacity obtained from the analytical approach. In order to attain a reliable comparison of the results obtained from the analytic and the finite element methods, in ABAQUS procedure the same elastic-ideally-plastic material is used as in the analytical calculations. The model of beam consists of quadrilateral shell elements.

The boundary conditions for the finite element analysis are defined by elimination of three degrees of freedom for each point located at the beam end. These constraints correspond to the support of the beam, which is assumed in analytical approach – Fig. 3a. This is in accordance with the Vlasov theory, because the

cross-section of a thin-walled beam behaves in its plane as a rigid frame and four non-collinear, parallel to beam axis constraints block warping (deplanation).

Figure 5 presents the deformations of the beam at the beginning of collapse. These deformations are not large what confirms that the analysis of limit state in the case of thin-walled beams can be based on the assumption of small displacements and small displacement gradients. This approach has been assumed in the present paper.

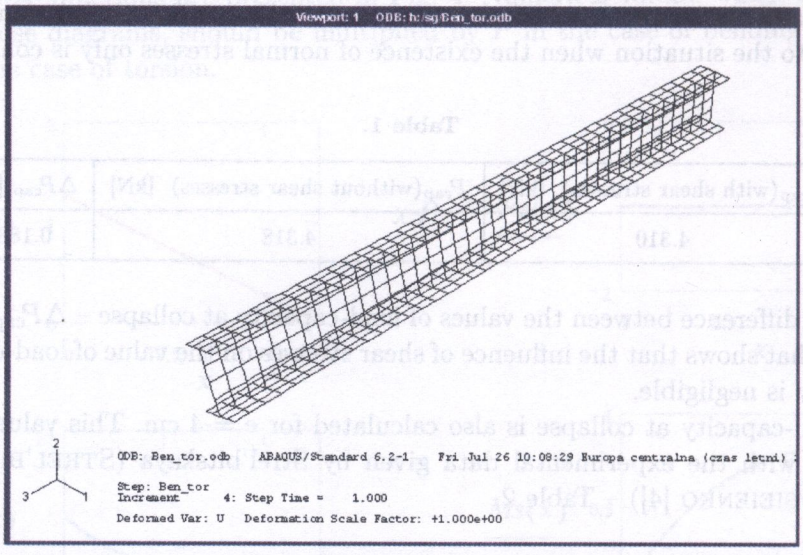

FIG. 5.

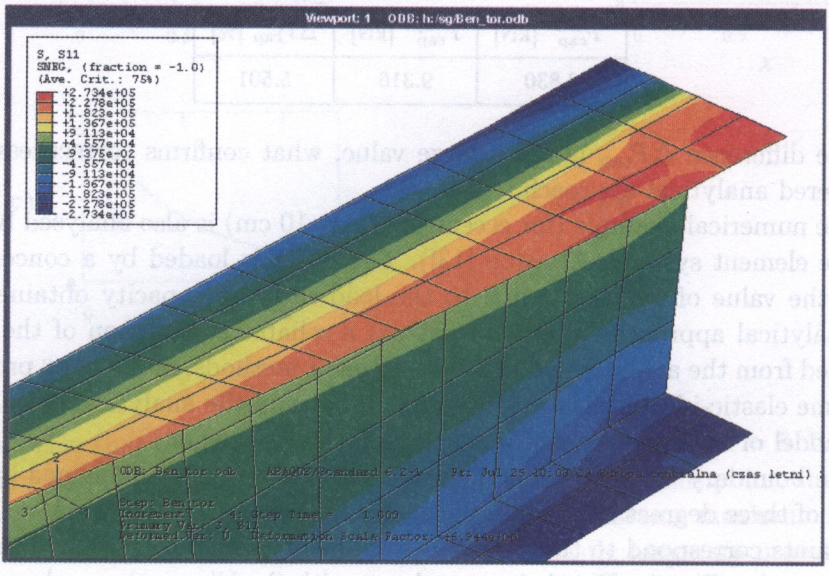

FIG. 6.

Picture 6 shows a view on the fixed end of the analysed beam, which corresponds to the place where plastic hinge appears. This figure presents the distribution of normal stresses. The regions where the yield stress $\sigma_Y = 231.4$ MPa is reached are indicated by the applied finite element procedure as the range of values equal to $227.8 \div 273.4$ MPa. It is visible that diagram of σ_x in the plastic hinge is very similar to the distribution assumed in analytic approach – Fig. 2a. It confirms that the model of plastic hinge in the analytical approach is built correctly.

Figure 7 presents the distribution of equivalent plastic strains at fixed end of the considered beam. This picture shows the shape of yielding zones. Yielding does not cover all the width of flanges what proves that the values of load-capacity at collapse obtained in analytical assessment are lower estimates. Indeed, the considered analytic procedure provides the values lower than the real values of load-carrying capacity, because it is a static approach.

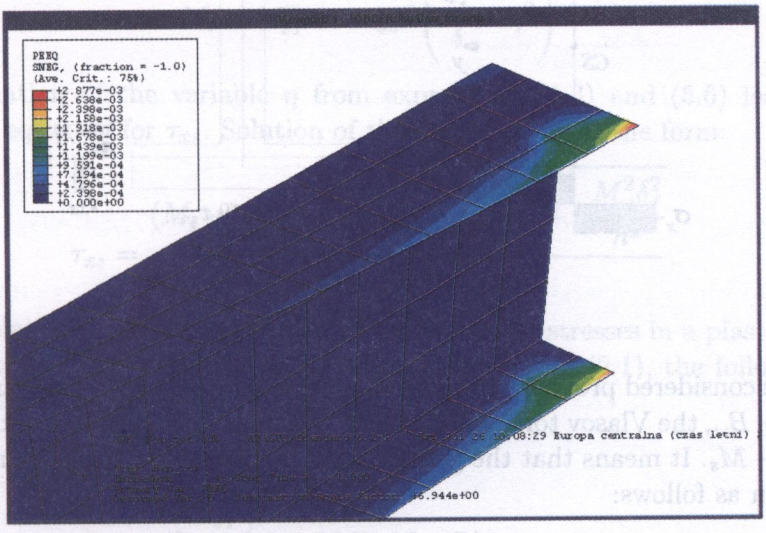

FIG. 7.

5. INTERACTION SURFACE FOR TORSION OF I-SECTION THIN-WALLED BEAM

In this case, while deriving the interaction surface formula, the same assumptions are used as in the first problem analysed. Only a model of plastic hinge is specified for the new loading conditions. The new diagrams of the distribution of normal and shear stresses in a plastic hinge for the analysed problem are presented in Fig. 8.

Normal stresses σ_x exist only in flanges and have antisymmetric distribution, what is confirmed by the diagram of these stresses in elastic state. The total shear

stresses distribution is composed of the average value along the cross-section thickness, produced by the Vlasov torsional moment, and of the antisymmetric part generated by the Saint–Venant torsional moment. In the case of I-section, the stresses in the web are created only by the Saint–Venant moment. It causes that full plastic state in web is achieved by antisymmetric limit shear stresses distribution – Fig. 8b, and interaction takes place only in the flanges. The quantity τ_Y denotes the shear yield limit and in accordance with the Huber–Mises–Hencky yield criterion, it is equal to $\sigma_Y/\sqrt{3}$.

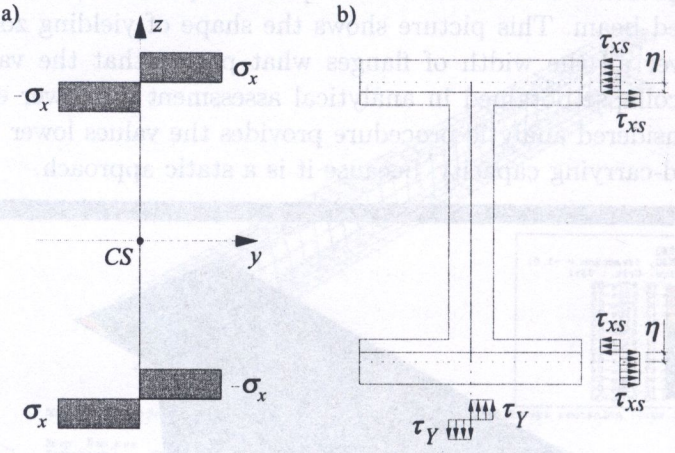

FIG. 8.

In the considered problem, three cross-sectional forces exist. They are: the bimoment – B_ω, the Vlasov torsional moment – M_ω and the Saint–Venant torsional moment – M_s. It means that the general form of interaction surface formula can be written as follows:

$$f(B_\omega, M_\omega, M_s) = 1. \tag{5.1}$$

Algorithm of deriving of interaction surface formula is identical to that used for the previously analysed problem. Analysis of normal stresses is very simple, because only the bimoment generates σ_x. In this case, using the equivalence relation (3.2) for stress distribution which is presented by Fig. 8a, leads to:

$$\sigma_x = \frac{B_\omega}{\frac{hb^2}{4}\delta_f}. \tag{5.2}$$

In the case of the shear stress analysis, the equivalence relations for M_ω and M_s should be written. In the considered case expression (3.7) assumes the form:

$$M_\omega = 2\tau_{xs} hb\eta. \tag{5.3}$$

The equivalence relation for the Saint–Venant torsional moment is derived for flanges and web, separately. It enables to derive the interaction surface formula only for flanges, which due to (3.9) reads

$$M_s^f = 4\tau_{xs} b \left(\frac{\delta_f^2}{4} - \eta^2 \right). \tag{5.4}$$

For the web, relation (3.9) takes form

$$M_{sY}^w = \tau_Y \frac{h\delta_w^2}{2}. \tag{5.5}$$

Index Y in (5.5) means that the full plastic state in the web is created only by the Saint–Venant torsional moment. Total Saint–Venant torsional moment M_s consists of M_s^f and M_{sY}^w. Then due to (5.4) we have

$$M_s - M_{sY}^w = 4\tau_{xs} b \left(\frac{\delta_f^2}{4} - \eta^2 \right). \tag{5.6}$$

Elimination of the variable η from expressions (5.3) and (5.6) leads to a quadratic equation for τ_{xs}. Solution of this equation takes the form:

$$\tau_{xs} = \frac{(M_s - M_{sY}^w) + \sqrt{(M_s - M_{sY}^w)^2 + 4\dfrac{M_\omega^2 \delta_f^2}{h^2}}}{2b\delta_f^2}. \tag{5.7}$$

The relations (5.2) and (5.7) describe the state of stresses in a plastic hinge. If these equations are substituted to the yield criterion (2.1), the following interaction surface formula will be derived:

$$\frac{B_\omega^2}{B_{\omega Y}^2} + \frac{(M_s - M_{sY}^w)^2}{2\left(M_{sY}^f\right)^2} + \sqrt{\frac{(M_s - M_{sY}^w)^4}{4\left(M_{sY}^f\right)^4} + \frac{M_\omega^2}{M_{\omega Y}^2}\frac{(M_s - M_{sY}^w)^2}{(M_{sY}^f)^2} + \frac{M_\omega^2}{M_{\omega Y}^2}} = 1, \tag{5.8}$$

where:

$B_{\omega Y} = \sigma_Y \dfrac{hb^2}{4}\delta_f$ – limit value of bimoment,

$M_{sY}^f = \tau_Y b \delta_f^2$ – limit value of the Saint–Venant moment – for flanges,

$M_{\omega Y} = \tau_Y hb\delta_f$ – limit value of the Vlasov moment.

Equation (5.8) presents the interaction surface, which is depicted in Fig. 9.

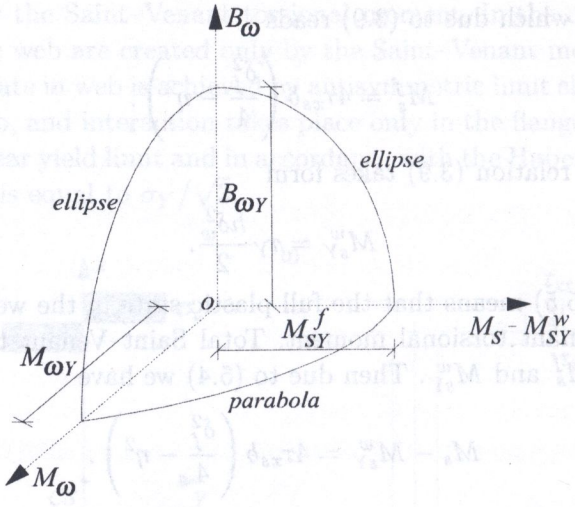

FIG. 9.

6. NUMERICAL EXAMPLE – TORSION OF AN I-SECTION THIN-WALLED BEAM

The beam, which is shown in Fig. 10a, will be analysed. The numerical data for this example are presented below:

Data: Length of beam: $L = 2\,\text{m}$, material constants: $E = 210\,\text{GPa}$, $G = 80\,\text{GPa}$, $\nu = 0.3$, dimensions of cross-section – Fig. 10b: $h = 19\,\text{cm}$, $b = 10\,\text{cm}$, $\delta_f = 1\,\text{cm}$, $\delta_w = 1\,\text{cm}$, yield stress: $\sigma_Y = 240\,\text{MPa}$.

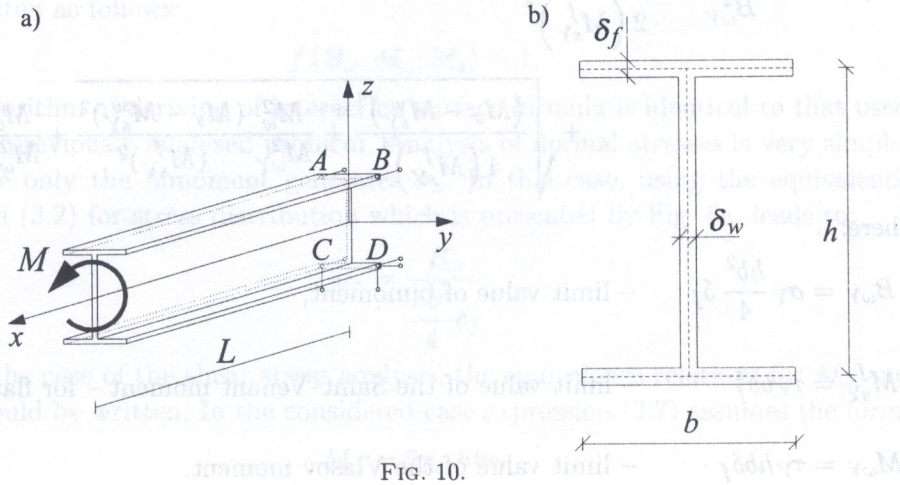

FIG. 10.

Algorithm of determination of the load-capacity at collapse is the same as in the analysed case of the beam subject to bending and torsion. It means that first of all, the most exerted cross-section should be found. Diagrams of B_ω, M_ω and M_s have the same shapes as in the first numerical example considered, what means that the most loaded cross-section is located at the fixed end of the beam. It is visible that a plastic hinge appears for variable x equal to zero.

Particular values of the cross-sectional forces on the fixed end of beam are presented by (6.1):

$$B_\omega(0) = 0.5766M, \qquad M_\omega(0) = M, \qquad M_s(0) = 0. \tag{6.1}$$

The Saint–Venant torsional moment is equal to zero, so in this case, the interaction surface formula (5.8) reduces to a simple form:

$$\frac{B_\omega^2}{B_{\omega Y}^2} + \frac{M_\omega^2}{M_{\omega Y}^2} = 1. \tag{6.2}$$

Substitution of numerical data to Eq. (6.2) and its solution leads to determination of the value of load-carrying capacity at collapse for the considered example. Additionally, the load-carrying capacity, but in the case when shear stresses are omitted, is calculated. Both values and difference between them are given in the Table 3.

Table 3.

M_{cap}(with shear stresses) [kNm]	M_{cap}(without shear stresses) [kNm]	ΔM_{cap} [%]
1.971	1.977	0.286

The quantity ΔM_{cap} is very small, what proves that the load-carrying capacity for thin-walled beams can be determined neglecting the shear stresses.

In the presented numerical example also the finite element system (ABAQUS [13]) is used. The finite elements model of the beam is identical as in the first analysis.

As it is shown in Fig. 11, the deformations at the beginning of the collapse process are not large, what confirms that the formulae, which are based on the assumption of small displacements and small displacement gradients, can be used in the limit analysis of thin-walled beams.

Figure 12 presents the diagram of normal stresses in a plastic hinge. The region of the beam where stresses attain the limit value 240.0 MPa are presented by ABAQUS calculations as zones in the $220.3 \div 264.4$ MPa interval. This diagram resembles Fig. 8a, what indicates that the model of plastic hinge assumed above is correct.

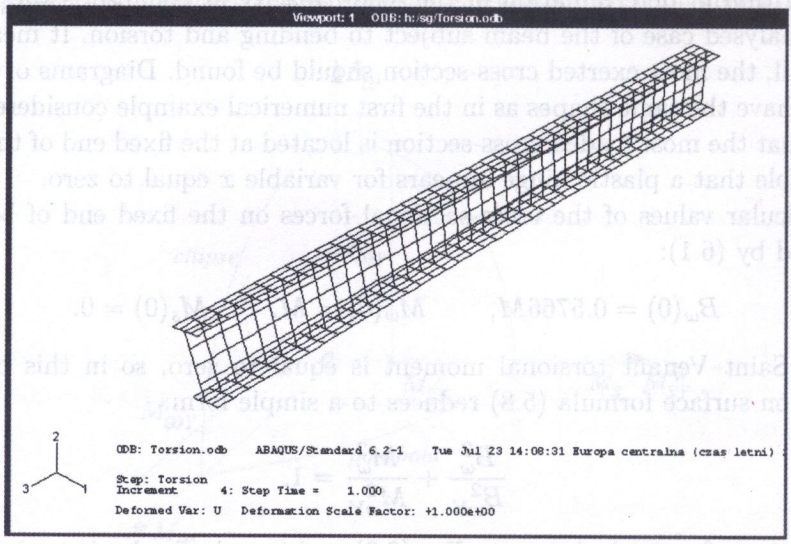

FIG. 11.

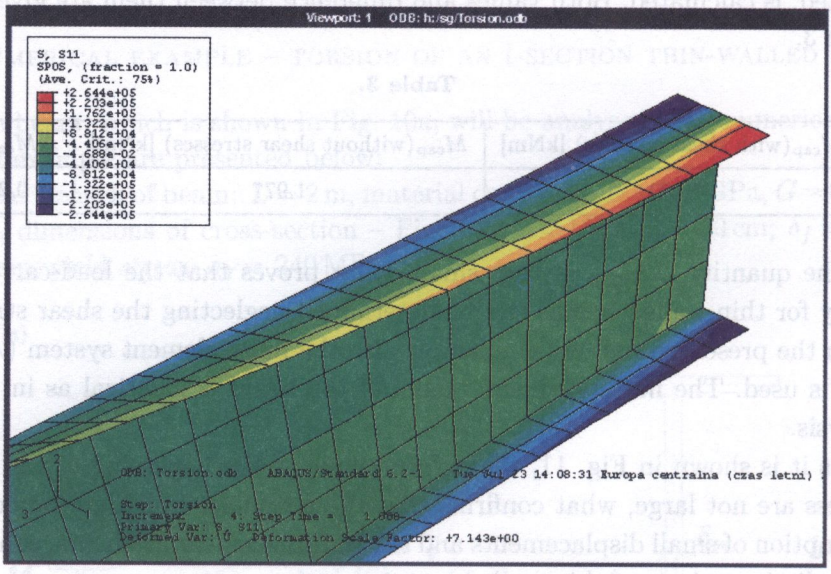

FIG. 12.

Similarly, to the case of bending and torsion of a beam, also the present diagram of equivalent plastic strains Figure 13, shows that the considered analytical approach describes the limit state with incomplete plastic hinge. It is

seen that the yielding area does not occupy all cross-sections, what means that the obtained analytic values of load-carrying capacity are lower estimates.

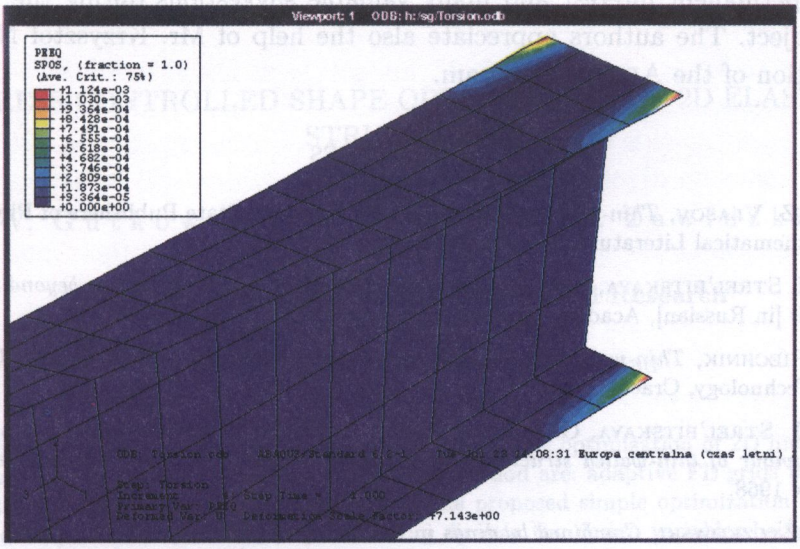

FIG. 13.

7. CONCLUSIONS

The paper presents an analytic method of determination of the load-capacity at collapse for an I-section thin-walled beam. The method is based on a static approach according to which the statically admissible stress distribution in the plastic hinge is assumed. The considered method deals with the interaction surfaces, which include (typical for the thin-walled beam theory) cross-sectional forces as bimoment. The presented analysis comprises deriving the interaction surface formulae for two kinds of load: torsion and bending with torsion. The analytical solution of examples shows the algorithm of calculation of load-carrying capacity for thin-walled beams. Comparison of analytical solutions with numerical and experimental data confirms the assumed hypotheses concerning the statically admissible distribution of stresses in the plastic hinge. Additionally, the obtained results show that the bimoment and bending moment have the decisive influence on the value of load-capacity at collapse what will enable us in the future to omit the shear stresses in the analysis of the load-carrying capacity of thin-walled beams.

ACKNOWLEDGMENT

The authors would like to express their gratitude to professor Stefan Piechnik for his permanent interest and many valuable suggestions during the work on this subject. The authors appreciate also the help of Mr. Krzysztof Nowak in application of the ABAQUS program.

REFERENCES

1. W. Z. VLASOV, *Thin-walled elastic beams* [in Russian], State Publishers of Physical and Mathematical Literature, Moscow 1959.
2. A. I. STREL'BITSKAYA, *Investigation of the strength of thin-walled beams beyond the elastic limit* [in Russian], Academy of Science, Ukrainian S.S.R., Kiev 1958.
3. S. PIECHNIK, *Thin-walled beams with open cross-sections* [in Polish], Cracow University of Technology, Cracow 2000.
4. A. I. STREL'BITSKAYA, G. I. IEVSIEIENKO, *Experimental investigation of elastic-plastic behaviour of thin-walled structures* [in Russian], Academy of Science, Ukrainian S.S.R., Kiev 1968.
5. M. ŻYCZKOWSKI, *Combined loadings in the theory of plasticity*, PWN – Polish Scientific Publishers, Warsaw 1981.
6. J. HEYMAN, *Elements of the theory of structures*, Cambridge University Press, Cambridge 1996.
7. S. GAWŁOWSKI, S. PIECHNIK, *Thin-walled beam with open cross-sections as a Timoshenko bar*, Journal of Theoretical and Applied Mechanics, **2**, 39, 269–281, Warsaw, 2001.
8. K.-J. BATHE, P. M. WIENER, *On elastic-plastic analysis of I-beams in bending and torsion*, Computers & Structures, **17**, 5–6, 711–718, Pergamon Press Ltd., 1983.
9. E. RAMM, P. OSTERRIEDER, *Ultimate load analysis of three-dimensional beam structures with thin-walled cross sections using finite elements*, Stability of Metal Structures, 201–210, Paris, 1983.
10. B. A. IZZUDDIN, D. LLOYD SMITH, *Large-displacement analysis of elastoplastic thin-walled frames*, Journal of Structural Engineering, **122**, 8, 905–925, August 1996.
11. N. W. MURRAY, *Introduction to the theory of thin-walled structures*, Clarendon Press, Oxford 1986.
12. M. KOTEŁKO, *Plastic mechanisms of failure in thin-walled girders of iso- and orthotropic walls* [in Polish], Łódź University of Technology, Łódź 2000.
13. ABAQUS (standard) Reference Manuals ver. 6. 2001, Hibbitt, Karlsson & Sorensen, Inc. Providence, 2001.

Received November 11, 2002.